Bachelor Thesis

Biomedical Engineering

A Methodology of Segmentation: Defining Adipose and Non-Adipose Tissue Volumes in Female Breast MR Images

Lonneke Heerkes

s2591189

July 1, 2024

Bachelor Thesis Committee:
Chair: Prof. Dr. Ir. N. Bosschaart
Daily supervisor: A. Boamfa MSc
External member: Dr. Ir. F.F.J. Simonis

Biomedical Photonic Imaging
Faculty of Science and Technology
University of Twente

UNIVERSITY OF TWENTE.

BMPI
BIOMEDICAL PHOTONIC IMAGING

ABSTRACT

Breastfeeding offers significant health benefits for both mothers and infants, supported by breast milk's unique antibodies and nutrients [1, 2]. The World Health Organization recommends exclusive breastfeeding for the first six months, followed by continued breastfeeding alongside complementary foods for up to two years [3]. Despite these benefits, breastfeeding initiation rates among Dutch women decline significantly from 69% postpartum to 19% at six months, with perceived insufficient milk supply cited as the primary challenge [4, 5].

Understanding the anatomical and physiological factors influencing lactation is important. This study focuses on breast segmentation to receive ratios of the adipose and non-adipose tissue in the mammary breast tissue. This study uses T2-Dixon Fat and Water scans acquired with a 1.5T MRI scanner from four subjects, one of whom is lactating. The created method to segment adipose and non-adipose tissue in the mammary breast starts with setting ellipses and points on five dispersed slices to remove non-mammary breast tissue. The breast's boundary is defined ventrally to the pectoralis major muscle, with lateral fat tissue delineated using established landmarks. The intermediate slices are interpolated using a 'spline' function in MATLAB.

The MATLAB Toolbox 'Medical Image Labeler' and a custom automated algorithm further distinguish adipose and non-adipose tissues. Segmentation results in a maximum variance of 6.69% in adipose tissue and 1.51% in non-adipose tissue, showing methodological consistency. The algorithms can be improved to prevent double-labeled tissue and not-labeled tissue within mammary breast tissue.

This method yields realistic volume calculations for adipose and non-adipose tissues together, validated against a comparative segmentation method using the same dataset. Variances range from 0.15% to 14.4%, underscoring the method's reliability and potential for advancing breast tissue analysis.

SAMENVATTING

Borstvoeding biedt aanzienlijke gezondheidsvoordelen voor zowel moeders als zuigelingen, ondersteund door de unieke antilichamen en voedingsstoffen van moedermelk [1, 2]. De Wereldgezondheidsorganisatie beveelt exclusieve borstvoeding aan gedurende de eerste zes maanden, gevolgd door voortzetting van de borstvoeding naast aanvullende voeding gedurende maximaal twee jaar [3]. Ondanks deze voordelen daalt het borstvoedingspercentage onder Nederlandse vrouwen aanzienlijk van 69% postpartum naar 19% bij zes maanden, waarbij onvoldoende melkproductie als belangrijkste uitdaging wordt genoemd [4, 5].

Inzicht in de anatomische en fysiologische factoren die lactatie beïnvloeden is belangrijk. Deze studie richt zich op het definiëren van de borst om de samenstelling van de adipose en niet-adipose weefsel te bepalen. Dit onderzoek maakt gebruik van T2-Dixon Vet- en Waterscans die zijn verkregen met een 1,5T MRI-scanner bij vier proefpersonen, waarvan er één borstvoeding geeft. De gecreëerde methode om vetweefsel en niet-vetweefsel in de borst te segmenteren begint met het instellen van ellipsen en punten op vijf verspreide plakken om niet-borstweefsel te verwijderen. De grens van de borst wordt ventraal aan de pectoralis major spier gedefinieerd en het vetweefsel aan de zijkanten wordt afgebakend met behulp van vaste herkenningspunten. De tussenliggende plakjes worden geïnterpoleerd met behulp van een 'spline'-functie in MATLAB.

De MATLAB Toolbox 'Medical Image Labeler' en een zelf-gemaakte geautomatiseerd algoritme kleurt vetweefsel en niet-vetweefsel. Segmentatie resulteert in een maximale variantie van 6,69% in vetweefsel en 1,51% in niet-vetweefsel. De algoritmes kunnen worden verbeterd om dubbel gelabeld weefsel en niet-gelabeld weefsel binnen borstweefsel te voorkomen.

Deze methode levert realistische volumes op voor vetweefsel en niet-vetweefsel samen, gevalideerd ten opzichte van een vergelijkende segmentatiemethode met dezelfde dataset. Varianties variëren van 0,15% tot 14,4%, wat de betrouwbaarheid van de methode en de mogelijkheden voor borstweefselanalyse versterkt.

CONTENTS

1 INTRODUCTION

Breastfeeding has many benefits for both the mother and infant in terms of physical and mental health [1]. Mother milk contains unique antibodies and nutrients that protect the newborn from infections and diseases [2]. Breastfeeding offers advantages for the mother, as it helps to reduce postpartum bleeding and lowers the risk of breast cancer [6]. Another benefit of breastfeeding is that it promotes the mother-infant relationship through maternal sensitivity and secure attachment [7]. Because of these reasons, the World Health Organisation recommends exclusive breastfeeding for at least the first six months, until two years of breastfeeding alongside other foods [3]. Research among Dutch women shows that 69% of all mothers starts breastfeeding after childbirth, after six months that percentage drops to 19% [4]. However, it is not a given that every mother wanting to breastfeed can do so. According to a research of 552 mothers, 7 out of 10 women encountered difficulties regarding breastfeeding [5]. The most reported difficulties are the perception of insufficient milk supply, cracked nipples, pain and fatigue. The first occurs in over a third of the mothers who participated in the research. Whether this perception is justified is often little known, because there is a lack of knowledge on the exact cause of lactation insufficiency. Therefore, it is important to learn more about the anatomical and physiological characteristics of the breast in relation to milk transfer.

To understand more about this, techniques will have to be applied to image the detailed structure inside the breast. A non-invasive and accessible way is Diffuse Optical Spectroscopy Imaging (DOSI). This imaging technique offers insights into the tissues in the lactating breast using near infrared light [8]. It allows tissue to be viewed up to 2cm inside the breast [9]. To validate if this 2cm is representable for the whole breast in terms of glandular and adipose tissue, and if it is correlated with the amount of extracted milk, Magnetic Resonance Imaging (MRI) can be used [8]. MRI is a precise, non-invasive imaging technique to distinguish various tissues [10].

In exploring the issue of lactation insufficiency, the following question arises: How can mammary breast tissue be segmented to quantify adipose and non-adipose tissue volumes separately based on MR imaging?

Answering this research question requires addressing the following sub-questions first.

- How is breast tissue defined regarding anatomical boundaries and differentiation from surrounding tissues?
- What MRI segmentation method is suitable for quantifying adipose and non-adipose tissue in the mammary breast?
- What is the interperson repeatability of the proposed segmentation method?

2 THEORETICAL BACKGROUND

To understand the context of lactation insufficiency, the anatomy and physiology of the female breast is explained based on the existing literature. This is followed by a theoretical background on MRI and a basis for MR image segmentation specific to breast imaging.

2.1 The Female Breast

A woman's breast consists mainly of mammary gland tissue, adipose tissue and connective tissue [11]. In addition to these three main components, the breast includes blood vessels, lymph nodes and an areola on each breast with the nipple in the centre. The volume of the breast is determined by genetic factors and body weight [12]. These affect both the overall size and shape of the breasts. The breasts also vary in size relative to each other, with one breast often being larger or smaller than the other [13].

2.1.1 Breast Anatomy and Physiology

Fully developed glandular tissue consists of 15-20 lobes, each divided into approximately 20 to 40 lobules (see figure 2.1) [14]. A lobule consists of primary ducts with secondary and tertiary branches extending from the nipple [15]. The glandular tissue is surrounded by stromal, or connective, tissue. The stroma maintains the 3D position of the mammary gland and supports the tissue to develop and function.

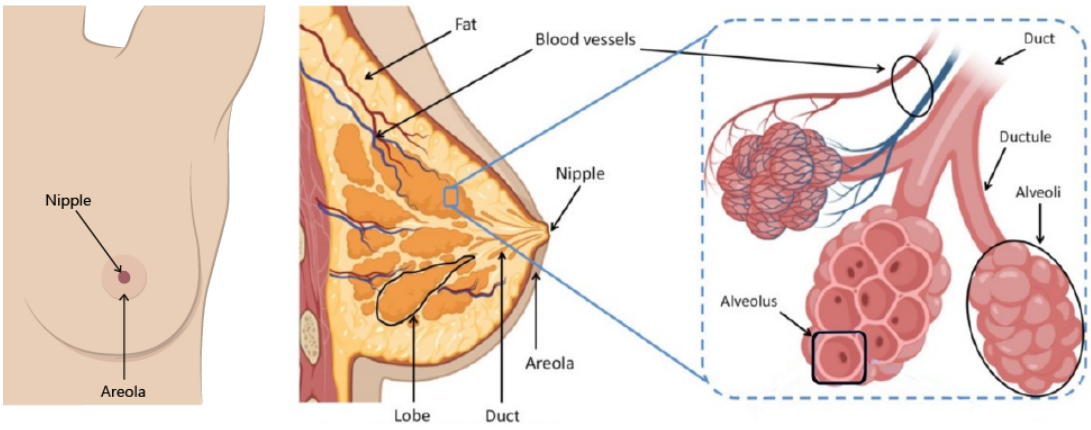

Figure 2.1: Mammary gland components [16]

During lactation, milk is produced and secreted in the alveoli by the glandular epithelial cells and myoepithelial cells, triggered by hormonal changes. When the myoepithelial cells release milk, the milk enters the alveolus. Each mammary gland comprises multiple alveoli, collectively referred to as a lobe. From the alveoli, the milk will travel through ductules before being secreted at the nipple (see figure 2.1) [16].

In the centre of the breast is a darker segmented area is located, also called the areola. Centrally located in the areola is the nipple, a protruding part from which the infant drinks breast milk. During pregnancy, the pigment of the nipple-areolar region gets darker and more elastic. The nipple-areolar region elongates around two times its resting length into a teat [17]. The areola is a slightly bumpy area that produces sebum which protects the area to keep it smooth and elastic. The autonomic nervous system is in control of the muscle fibers in the nipple and areola, which allows the nipple to erect when breastfeeding [18].

The arterial supply to the breast is primarily provided by 60 percent from the anterior and posterior medial branches and 30 percent from by the lateral mammary branch of the lateral thoracic artery. The remaining 10 percent is transported by smaller arteries including the posterior intercostal arteries and the pectoral branch of the thoracoacromial artery [19]. The larger veins follow the major arteries back towards the heart and the smaller veins spring radially from the nipple and flow into a periareolar vein. Between the two breasts, There is no symmetry in terms of arteries and veins between the two breasts.

2.1.2 Breast Definition

In the transverse plane of the MR images, three different muscles can be seen: the pectoralis major muscle, the serratus anterior muscle, and the latissimus dorsi muscle, as shown in figure 2.2. The breast is positioned ventrally to the pectoralis major muscle. Its tissue extends over the muscle, spanning vertically from approximately the second to the sixth rib. Horizontally, the breast extends from the sternum to the anterior aspect of the armpit [20].

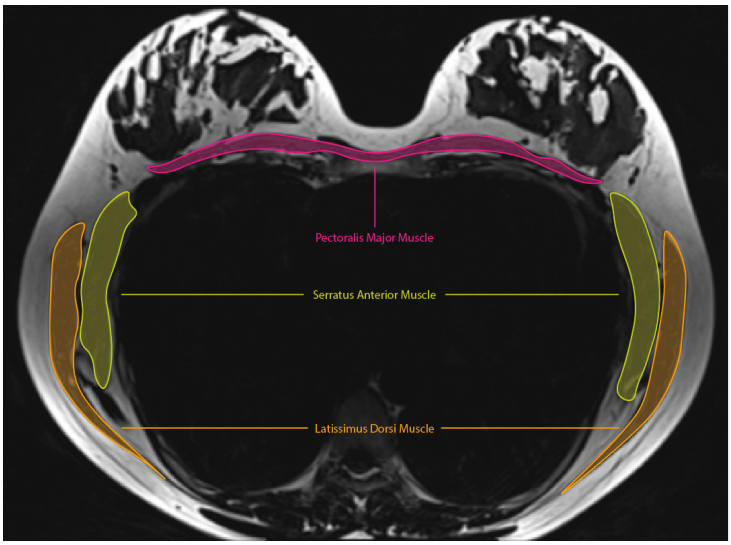

Figure 2.2: Muscles in the chest

The pectoralis major muscle does not separate the entire breast tissue from the rest of the body. On the lateral sides, breast adipose tissue overflows into fatty tissue that does not belong to the breast. At this point, there is no clear anatomical separation [21]. In the literature, a horizontal line is drawn on these lateral sides to delineate the boundary of the breast fatty tissue.

2.2 Female Breast Development

The development of the female breast begins in the fetus stage, during which it comprises two distinct parts. The epithelial parenchyma consists of ducts that branch off, leading to the development of secretory acini. The secretory acini are small saccular structures that are responsible for the production and secretion of milk during the lactation process. Thus, this first part of the breast is the functional part that consists of lobes, lobules and ductuses that produce, store and transport milk during lactation. Approximately 10% to 15% of the total volume of the breast is occupied by this part [14]. The second element is the stroma, which is the surrounding tissue of the parenchyma consisting of adipose tissue, connective tissue, blood vessels and nerves that support and nourish the breast. This component of the breast is responsible for providing shape and structural support [22].

At birth, only a few milk ducts are present, which remain underdeveloped until puberty. From puberty onwards, various hormones cause further differentiations of tissues in the breast, which will also cause the breast to enlarge. The main hormones involved are ovarian estrogen and progesterone [14].

During pregnancy, the breast achieves complete functionality and development. This development is stimulated by estrogen, progesterone, growth hormone, prolactin, and placental hormones. The result

of this development is that the overall volume and density of the breast increase [14]. It also develops the maximum viable alveoli, allowing for sufficient milk production and secretion for the infant [23]. When breastfeeding stops, the breast may undergo regression, with the possibility of this process repeating several times. Figure 2.3 illustrates the development of lobes and ducts through these different phases.

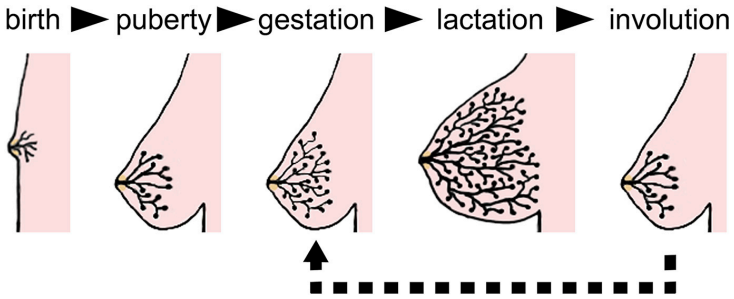

Figure 2.3: Development of the mammary gland [23]

2.2.1 Lactation

Lactation is the production and secretion of milk in the human breast, triggered by hormonal changes in the mammary glands. During the first couple of days after birth, the mammary glands produce colostrum. This is a yellowish fluid with more protein, vitamin A, antibodies and minerals and less lactose and fat compared to the milk produced later in the lactation period. Colostrum helps protect the baby against infection and gives the digestive system a good start. After two or three days, true milk production begins. Mechanoreceptors in the nipple send impulses to the hypothalamus when the infant is drinking. This stimulates the hypothalamus to secrete prolactin-releasing factors, leading to the actual release of prolactin, which stimulates the mammary gland to produce more milk [18].

2.3 Magnetic Resonance Imaging

MRI, Magnetic Resonance Imaging, is a technique that produces high-resolution, high-contrast cross-sectional images of the body [24]. Since the human body is composed of at least 60% of water, MRI will take advantage of the nucleus of hydrogen, protons [25]. The magnetic field inside the scanner tube affects the nuclear spin of proton molecules. When placed in a strong magnetic field, groups of protons, known as spin systems, can be stimulated into motion by applying radio frequency (RF) signals through wire coils surrounding the patient. When the RF pulse is not applied anymore, the protons excites energy which a receiver coil will detect. The receiver coil measures the time it takes for the hydrogen nuclei to return to their original position and also the amount of released energy [26]. A breast coil is made to get a clear image of the breast as it provides comfort, a good position of the breasts and a high resolution of the MR images [27].

The speed at which the nuclear spin of excited atoms returns to the ground state can characterize tissue properties and is referred to as the relaxation time, measured in both longitudinal (T1) and transverse (T2) directions. T1, or longitudinal relaxation time, describes the exponential recovery of the longitudinal magnetization (Mz) to its equilibrium value (M0). It is determined by changing the repetition time (TR) and is defined as the time at which 63% of the longitudinal magnetization has recovered. T2, or transverse relaxation time, describes the exponential decay of the transverse magnetization (Mxy) to zero due to random local interactions and dephasing of the spin system. It is measured by changing the echo time (TE) and is defined as the time at which 63% of the transverse magnetization has decayed. The T1 and T2 times are unique for each tissue, so MRI settings can be adjusted to show different types of tissues.

2.3.1 The Dixon Method

The Dixon method relies on the different frequencies of fat (F) and water (W) tissues during an MRI scan [28]. The technique involves the acquisition of two separate images using a modified spin echo pulse sequence [29]. One is a conventional spin echo image where the water and fat signals are in phase. The other is acquired with a slightly shifted readout gradient so that the water and fat signals are 180° out of phase. When signal vectors of protons are aligned in the same direction, an in-phase (IP) image is produced (see figure 2.4a). When these vectors of protons point opposite to each other, an opposed-phase (OP) image is created (see figure 2.4b). Mathematically (2.1, 2.2, 2.3, 2.4), the water only and fat only images can also be generated, as illustrated in figure 2.4c and figure 2.4d.

$$IP = W + F \tag{2.1}$$

$$OP = W - F \tag{2.2}$$

$$Water\_only \Rightarrow IP + OP = (W + F) + (W - F) = 2W \tag{2.3}$$

$$Fat\_only \Rightarrow IP - OP = (W + F) - (W - F) = 2F \tag{2.4}$$

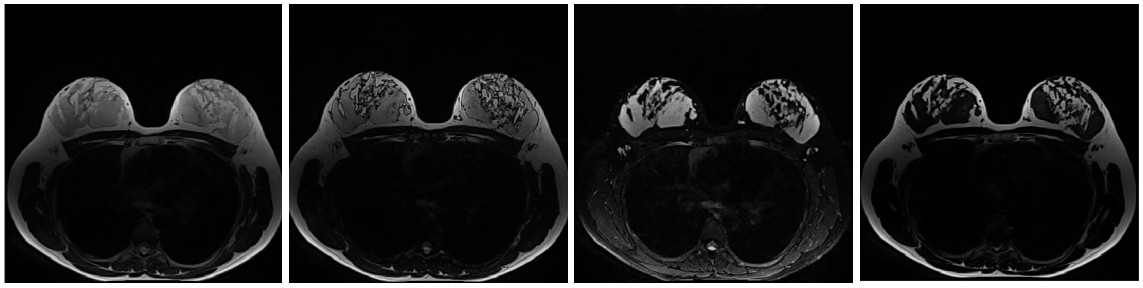

(a) In-phase (b) Opposed-phase (c) Water only (d) Fat only

Figure 2.4: Different types of MR Images of a lactating breast

3 MATERIALS AND METHODS

To segment the MR images, the correct settings of the MRI scanner and setup of the subject are essential. With this, the desired tissues can be visualized ultimately leading to more accurate results. The imaging sequence has been defined by previous research at the research group Biomedical Photonic Imaging (BMPI) in cooperation with the research group Magnetic Detection and Imaging (MD&I) at the University of Twente. Several breast MRI images were obtained between November 2023 and February 2024. These images will be used in this study.

3.1 Study Population

The women who participated in this study volunteered via the University of Twente website and are all not known to have breast anomalies. The group of women can be divided into two groups. The lactating women are known to be healthy, non-pregnant, between 18 and 45 years old and 0.5 to 12 months postpartum. The other group is the non-lactating group. These women are aged between 18 and 45 years, healthy, not pregnant and at least nine months postpartum. So far, there are 4 usable scans to use for this study, including one lactating woman and three non-lactating women. The information of the subjects can be seen in table 3.1.

Table 3.1: Personal data of the subjects

Subject	Body Weight [kg]	Lactating
1	65	No
2	70	Yes
3	60	No
4	75	No

3.2 Image Acquisition

In TechMed Centre at the University of Twente, the Siemens Magnetom Aera 1.5 Tesla MRI scanner (see Figure 3.1a) is used for this study. The subject is positioned prone on the Siemens breast 18 coil (see Figure 3.1b), with the head facing downwards on the headrest, the arms above the head, resting on the arm rests and the breasts placed in the two openings as shown in Figure 3.1c.

(a) 1.5T MRI-scanner (b) Breastcoil [30] (c) Position

Figure 3.1: Image setup

The subject lays for a period of 15 minutes in the MRI scanner, which offers the possibility of obtaining different MRI scans. Starting with the positioning scan, also called the localizer. After this scan, T1 and T2 Dixon scans IP and OP, are followed. In this study, only the T2 Dixon scans are used to determine the volume of the breast.

3.2.1 Acquisition Parameters

Table 3.2 shows the parameters used for the T2 Dixon scans.

Table 3.2: MRI acquisition parameters for the dataset of 4 subjects

Acquisition Parameter	Value
Magnetic Field Strength (T)	1.5
Repetition Time (ms)	4750
Echo Time (ms)	81
Slice Thickness (mm)	2
Pixel Spacing (mm^2)	0.9375 x 0.9375
Number of Slices	83

3.3 Defining Segmentation Method

In this project, a method is developed in MATLAB (r2024a) to segment the breast from the whole MRI image. The MATLAB toolbox 'Medical Image Labeler' is used to label adipose tissue and non-adipose tissue, consisting of glandular tissue and blood vessels.

3.4 Robustness of Segmentation Method

A protocol was written to test the segmentation on consistency, when it is performed by multiple individuals. Five protocol testers will use the protocol to segment the dataset of subjects 2 and 4.

3.5 Comparising Volume Results with Another Methodology

Parallel to this study, Rozan developed a method for measuring the total volume of mammary breast tissue. This method used the placement of five points that together form a smooth line along the Pectoralis Major Muscle. To remove the remaining fat tissue on the lateral sides of the body, the second part of the segmentation is done in the same way as the method developed in this study. The placement of these points are done on three different slices (beginning, middle, end) after removing slices from the DICOM

folder where no mammary breast tissue was visible. After this manual segmentation, a mask remains in which all pixels above a certain threshold are marked as mammary breast tissue.
In this study, the total volume of mammary breast tissue is not calculated, but by adding the adipose and non-adipose tissue together, this can be seen as the total volume of mammary breast tissue.

4 RESULTS

The result of this research is the self-designed method to segment breast tissue. The different components of this segmentation methodology are described and the manual part is tested by five protocol testers.

4.1 Segmentation of Mammary Breast Tissue

Starting the segmentation process of the breast, it is essential to define landmarks in order to segment the breast from the MR image. Several custom scripts are used in MATLAB with the Medical Image Labeler Toolbox. All the steps required to determine the volume of the labeled tissue are detailed in a flowchart. Additional explanation is needed to explain the different processes and sub-processes, so these are in the accompanying text.

4.1.1 Flowchart

The flowchart consists of different colored symbols. These have meanings, explained in the legend in Figure 4.1.

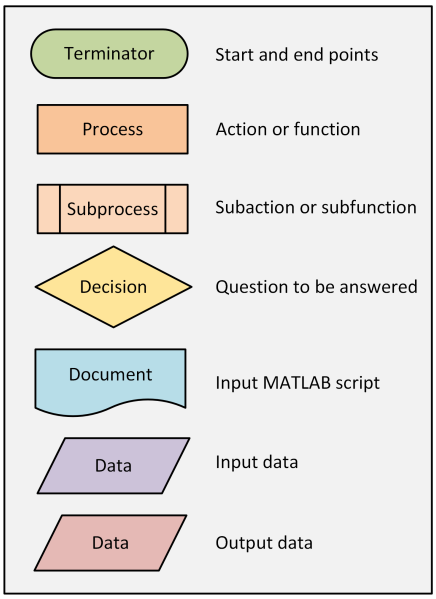

Figure 4.1: Flowchart legend

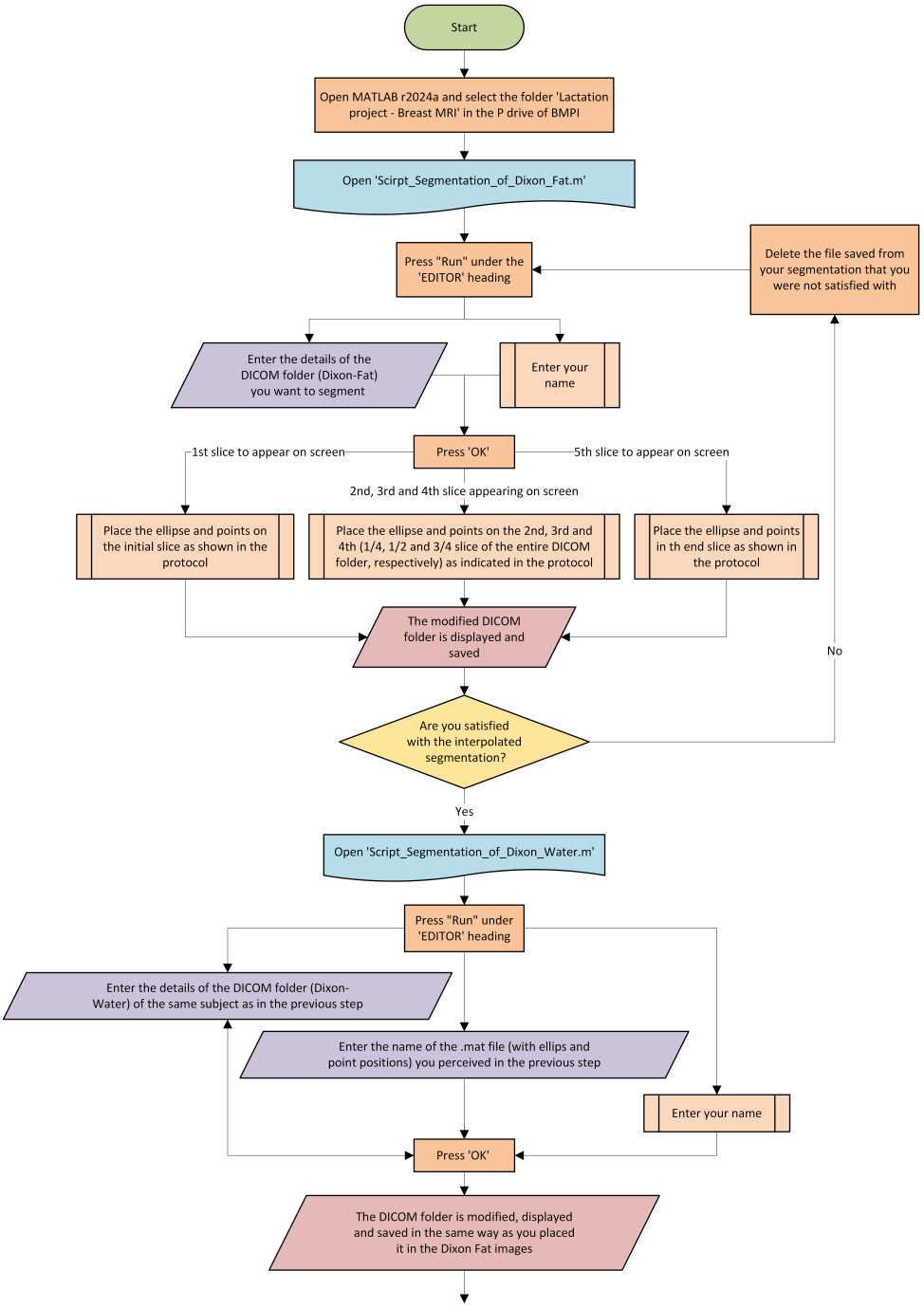

Figure 4.2: Segmentation of mammary breast tissue represented by a flowchart - part 1

The first part of the flowchart is shown above in Figure 4.2 and concerns the modification of the datasets, the Dixon-Fat DICOM folder and the Dixon-Water DICOM folder. The primary guideline for defining mammary breast tissue is the anatomical boundary between the mammary gland and the pectoralis major muscle. This principle should be taken into account when going through the first block of the three sub-processes. This boundary is easy to see on the Dixon-Fat images because the fat tissue is bright (high intensity) and the muscle tissue is dark (low intensity). For this reason, all images are labeled on the Dixon-fat images, which can later be used to determine the adipose tissue volume. To determine the volumes of adipose and non-adipose tissue, all non-breast tissue must be removed. This is done by setting the intensity of the non-breast tissue pixels to zero, making the pixel black. This mask of mammary breast tissue is saved and can be reused on the Dixon-Water images to define the volume of the non-adipose tissue.

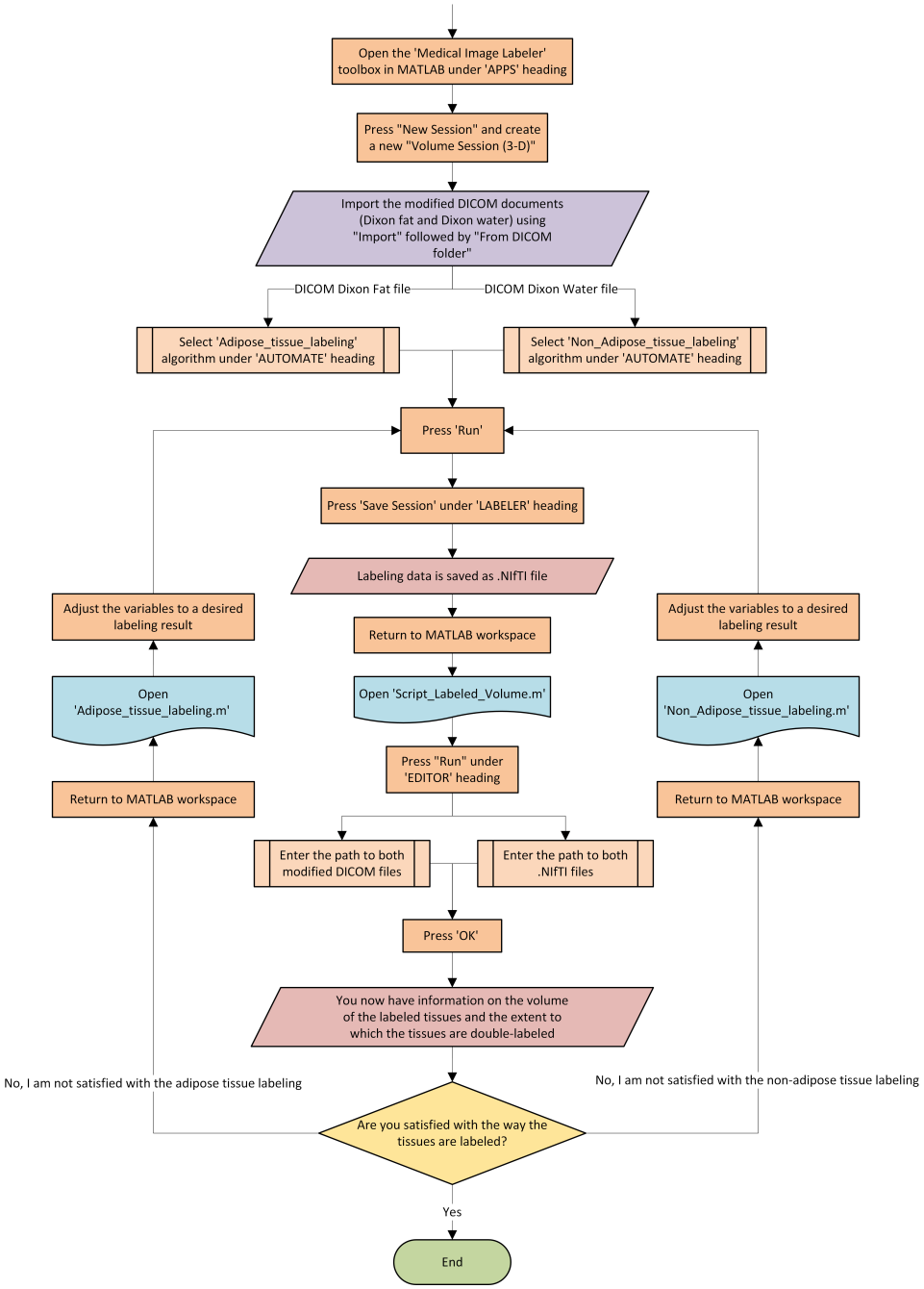

Figure 4.3: Segmentation of mammary breast tissue represented by a flowchart - part 2

The steps to label the tissue and determine volumes are shown in the second part of the flowchart, shown in Figure 4.3. Tissue labeling is done in a MATLAB toolbox called 'Medical Image Labeler'. This toolbox uses automated algorithms based on threshold and contouring values that can label adipose and non-adipose tissue. The results are immediately visible in different cross-section images and in a 3D figure.

As a final step, a MATLAB script can be used to upload the labeling information to determine the volumes of adipose and non-adipose tissue. This also shows the ratio between the two tissues and whether any pixels are labeled as both types of tissue.

4.1.2 Masking Mammary Breast Tissue

The mammary breast tissue must be masked manually. The first step is to draw an ellipse across the chest in the transverse plane, to give all pixels in the ellipse an intensity of zero. This ellipse must run across three points, indicated by the orange points in figure 4.4. The outer two points are identified by a piece of fatty tissue located between the pectoralis major muscle and the serratus anterior muscle (shown in figure 2.2). The midpoint is located at the lowest central point on the skin between the two breasts.

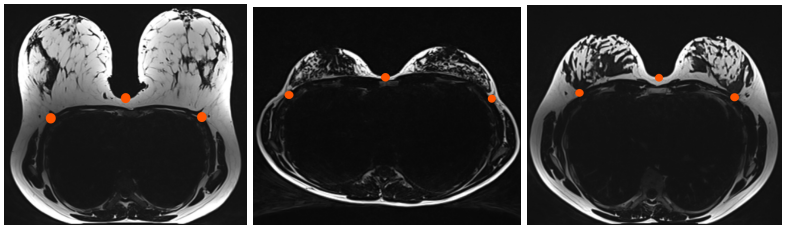

Figure 4.4: Breast definition pectoralis major muscle boundary

On the lateral position to the breast, adipose tissue changes into normal fat tissue surrounding the chest. A boundary must be manually drawn to determine whether or not fat tissue still belongs to the breast. In most cases, there is an indentation at this spot, where fatty tissue transitions occur (shown with a magenta-colored point in figure 4.5). This point is defined as the end of the lateral side of the mammary breast. In some slices of the MRI scans it is harder to define this indentation, as in figure **??**. In such cases, there is a segment that appears relatively straight. The point is then placed in the center of this segment. These points will be called A1 and A2, respectively.

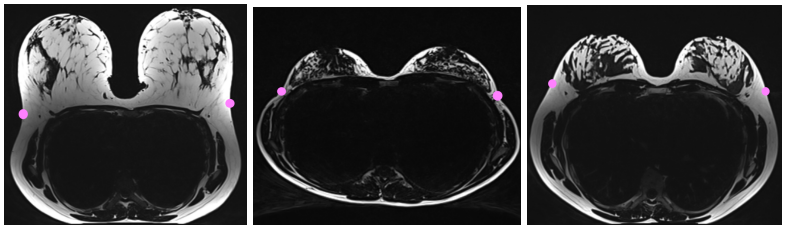

Figure 4.5: Breast definition on the lateral side of the breast

These points define a perpendicular line to the ellipse (see Figure 4.6a), using a formula in the script . The point where the lines are crossing the ellipse, are called B1 and B2 respectively. The left line creates a mask to its left, turning every pixel in this area black. Similarly, the right line creates a mask to its right, making every pixel in this area black. After applying all the masks (to the left of the left line, to the right of the right line and inside the ellipse), only the breast tissue remains visible, as seen in figure 4.6b.

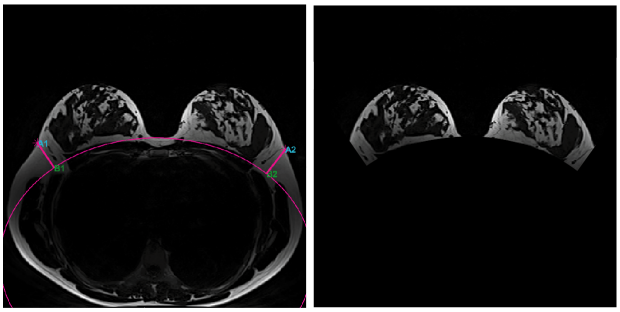

(a) During segmentation (b) After segmentation

Figure 4.6: Manual segmentation of breast tissue, during and after

4.1.3 Interpolation of Masked Areas

These ellipses and points need to be drawn on 5 different slices: the first slice, the slice at one-quarter, the middle slice, the slice at three-quarters and the last slice. The five manually segmented slices are used to interpolate the segmentation to all slices. The first interpolation involves the ellipses, which will be based on their central points, widths, and heights. The second interpolation concerns points A1 and A2; these points will be interpolated separately, allowing a line to be drawn between these points on every slice. Similarly, the third interpolation will be for points B1 and B2. To ensure smooth interpolation that follows the natural anatomical lines of the body in the sagittal plane, the 'spline' function in MATLAB WILL be used. The 'spline' function generates smooth, curved lines that pass through a set of given points. The results of this interpolation are shown in figure 4.7. In these figures, only the middle slice (slice 42) is drawn by hand, the other six are based on the interpolation technique (based all the five manually drawn ellipses and points).

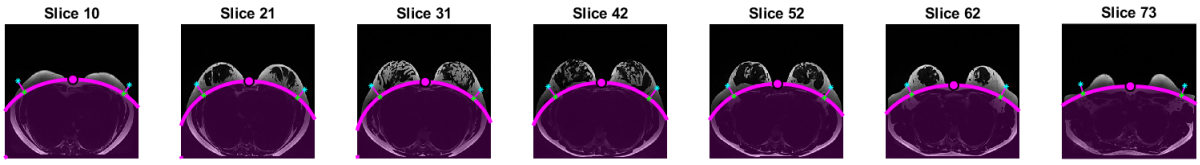

Figure 4.7: First step of segmentation on subject 2, Dixon Fat Images

The interpolated results of the other three subjects can be seen in appendix A.

Once the manual segmentation of the T2 Dixon Fat images is completed, all the positional data of points and ellipses are saved. These saved coordinates of the ellipses and points in each slices can be loaded into another MATLAB script to perform the segmentation the T2 Dixon Water images, these results are shown in figure 4.8. Following this process, two modified DICOM folders will be generated and ready for the labeling adipose and non-adipose tissue.

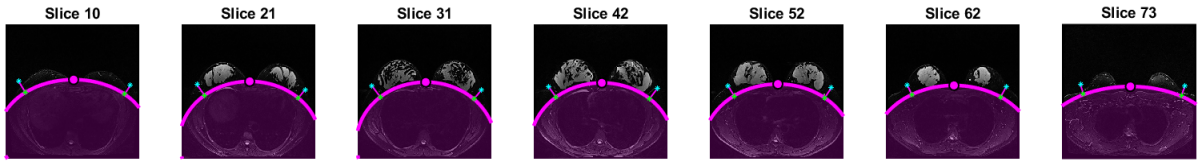

Figure 4.8: First step of segmentation on subject 2, Dixon Water Images

The interpolated results of the other three subjects can be seen in appendix B.

4.1.4 Tissue Labeling

The second part of this segmentation process will be conducted using the MATLAB Toolbox: Medical Image Labeler. Specifically, there are two distinct algorithms: one for labeling adipose tissue and another for labeling non-adipose tissue (glandular tissue and blood vessels). These algorithms are based on specific threshold and contour values. The values of these variables can be adjusted, to label as correct as possible. In this toolbox, the DICOM folders can be loaded and the algorithms applied. This labeling can then be checked in different planes and a 3D Image. These results are shown in Figure 4.9 and 4.10.

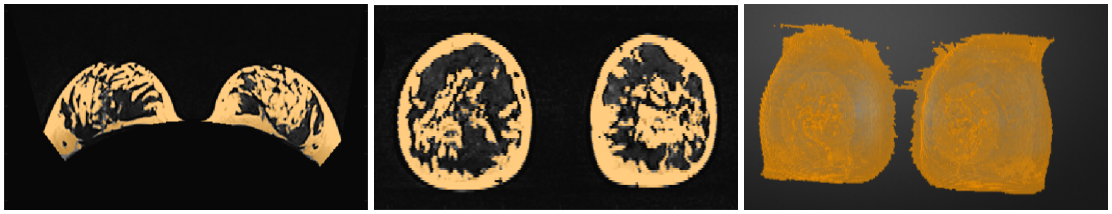

(a) Transversal plane (b) Coronal plane (c) 3D image

Figure 4.9: Labeled adipose tissue of subject 2, Dixon Fat Images

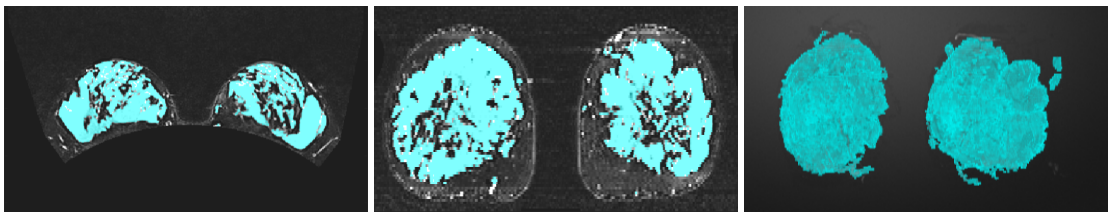

(a) Transversal plane (b) Coronal plane (c) 3D image

Figure 4.10: Labeled non-adipose tissue of subject 2, Dixon Water Images

4.1.5 Volume of the Labeled Tissues

The labeled tissue is saved as a NIfTI file and can be loaded into the created MATLAB script. From the modified DICOM folder, the slice thickness and pixel spacing can be extracted to calculate the volume of the labeled tissue. This is done by multiplying the number of labeled pixels by the slice thickness and pixel size, resulting in the values shown in table 4.1. The results presented are averaged after performing the full segmentation three times.

Table 4.1: Volumes of adipose and non-adipose tissue of subjects 1-4, tested 3 times by the same person

Subject	Mean Volume of Adipose Tissue (L)	Mean Volume of Non-Adipose Tissue (L)
1	0.5217	0.1440
2	0.9374	0.5765
3	0.3702	0.3478
4	3.3988	0.5521

4.1.6 Double labeling

To check if the results above are reliable, the NIfTI files of the Adipose Tissue and Non-Adipose tissue of the same subject are compared to each other. The result of this is placed in figures 4.11 (a-d) below. In orange the adipose tissue is labeled, non-adipose tissue in blue and the double-labeled pixels in red. A total 100% is together the Adipose tissue, Non-Adipose tissue and the double-labeled tissue (counted as a single pixel, not double). Some pixels were labeled twice in all subjects. This means that the volumes of adipose tissue and/or non-adipose tissue are shown in table 4.1 are too high, because a pixel can only have one type of tissue labeling.

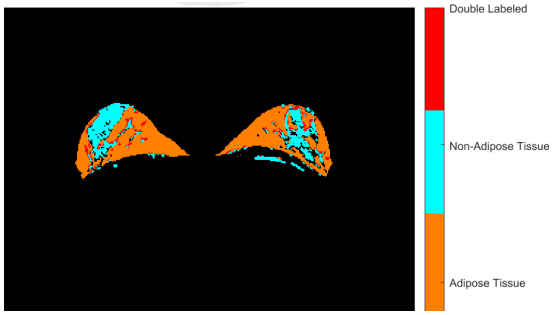

(a) Subject 1:
Percentage voxels adipose tissue only: 77.15%
Percentage voxels non-adipose tissue only: 17.16%
Percentage voxels in both files: 5.69%

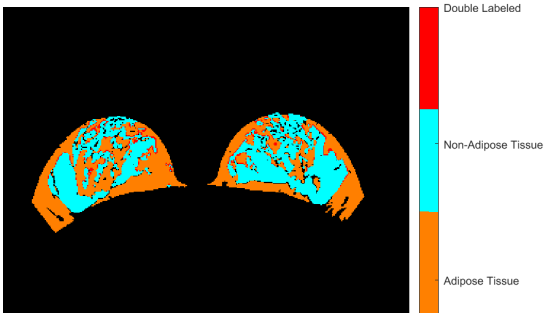

(b) Subject 2:
Percentage voxels adipose tissue only: 60.21%
Percentage voxels non-adipose tissue only: 35.95%
Percentage voxels in both files: 3.84%

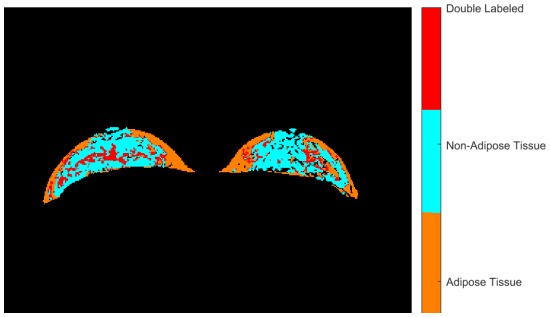

(c) Subject 3:
Percentage voxels adipose tissue only: 44.84%
Percentage voxels non-adipose tissue only: 41.41%
Percentage voxels in both files: 13.75%

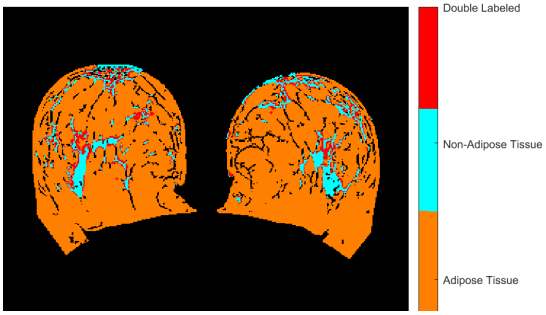

(d) Subject 4:
Percentage voxels adipose tissue only: 85.05%
Percentage voxels non-adipose tissue only: 8.04%
Percentage voxels in both files: 6.91%

Figure 4.11: Labeled tissues, including the double-labeled tissue in red

4.2 Test of Protocol

The manual segmentation is tested on five different protocol testers. For this test, a protocol is made (shown in Appendix C). The resulting volumes of the adipose and non-adipose tissue of subject 2 and 4 are shown in Figure 4.12

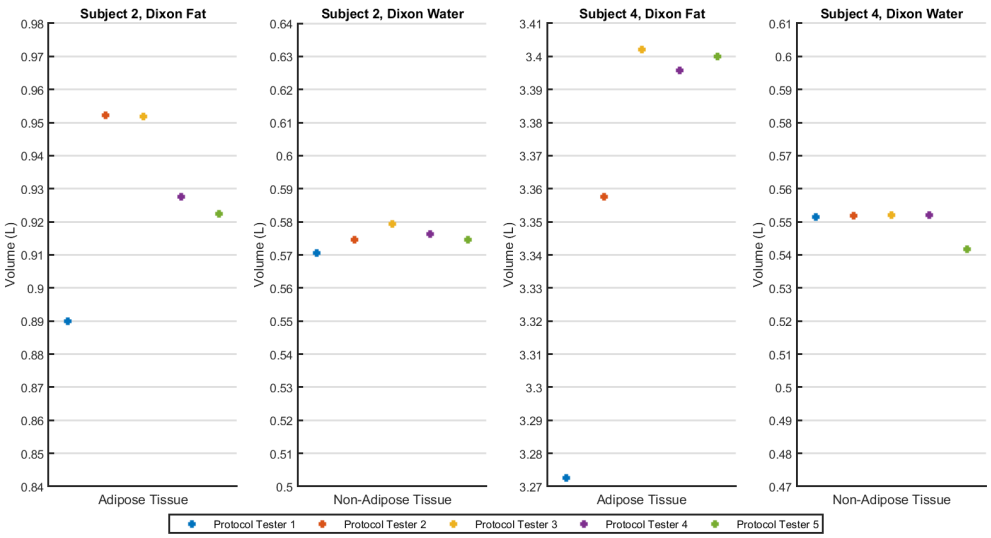

Figure 4.12: Volumes received from the protocol testers

Table 4.2 summarises statistical measures including mean, range, variance and standard deviation to analyze the results on the volumes from received from the five protocol testers. The mean shows the average measurement per tissue type and subject. The range shows the difference between the highest and lowest values. The variance is adjusted by the mean, indicating measurement consistency. Here it is noticeable that the outcomes are higher in adipose tissue than in non-adipose tissue. The standard deviation shows how measurements vary from the mean. Again, the outcomes are higher in adipose tissue compared to non-adipose tissue.

Table 4.2: Test results of the protocol

Dataset	Mean (L)	Range (L)	Variance (%)	Standard deviation
Subject 2, Adipose Tissue	0.928212	0.06216	6.69	0.0256
Subject 2, Non-Adipose Tissue	0.575072	0.0087	1.51	0.0032
Subject 4, Adipose Tissue	3.3656	0.1294	3.85	0.0551
Subject 4, Non-Adipose Tissue	0.549624	0.0103	1.87	0.0045

4.3 Comparison of Segmentation Methods

Table 4.3 shows the results of the average volumes of the method from this study compared with the average volumes from Rozan's parallel study. The total volume was obtained by adding the adipose tissue to the non-adipose tissue. The highest variance is in the dataset of subject 2 and the lowest in the dataset of subject 4.

Table 4.3: Comparison, with the parallel study, of the total volume of the mammary breast

Subject	Volume (this research) (L)	Volume (parallel research) (L)	Range (L)	Variance (%)
1	0.6656	0.7394	0.0738	10.5
2	1.513	1.743	0.23	14.4
3	0.7180	0.7934	0.0754	9.96
4	3.950	3.956	0.006	0.15

5 DISCUSSION

5.1 Segmentation of Mammary Breast Tissue

The literature has shown that the mammary breast tissue is delineated at abrupt points. Therefore, this research has created a new method using MATLAB, mainly used at the University of Twente, making it relatively accessible for implementation for further research.

5.1.1 Manual part to mask the Mammary Breast Tissue

This study shows a method to segment the female breast, in order to get the (tissue) volumes of the breast. Since there is not an anatomical boundary of the breast, this has to be drawn in manually. Several options have been tried to black out all the non-breast tissue in the images. A straight line or a curved line were both options for the first step of segmentation. However, a straight line was often not accurate enough, removing too much or too little of the breast tissue. The natural shapes of the body cannot be compared to a straight line. From there, the curved line was being considered. Points could be drawn in at various landmarks, which eventually would connect with a line. The disadvantage of this is that you do not know in advance how the line will curve using the spline function in MATLAB. Therefore, an ellipse chosen to use for the first step of segmentation. An advantage of using an ellipse is that it allows for the visualization of the cut-off area in advance, showing how the curve of the ellipse will be shaped.

The second step in the manual segmentation process offers room for improvement. In the first and last few slices of the DICOM folder, no breast tissue is shown. Points A1 and A2 placed on the first slice and last slice are placed at points where they will minimise the interpolation draw to points where it would not be expected. This is not the best way to handle this. Therefore, A1 and A2 should no longer be drawn in at the begin and end slice. Only at a quarter, half and three-quarters. To still include the extreme slices, an extrapolation method on points A1 and A2 can be used.

The time it takes to do this segmentation by hand, is mainly dependent on experience. The protocol testers were already several minutes faster on the second segmentation, only with one dataset of experience. The protocol is sensitive to errors. If the protocol tester is not satisfied with an insertion of an ellipse or point, the process has to start all over again. An improvement to the script would be to then only redo that slice. In addition, drawing in points A1 and A2 is sometimes difficult to see because the MRI images are often dark and the cursor of the points are also indicated with dark lines. This makes it more difficult to click on the correct points of A1 and A2. A final aspect where the time of the manual segmentation method may differ is the location from which the DICOM folder is loaded. If they are located in a protected folder on the drive, the script may take up to five minutes longer.

5.1.2 Interpolation of Masked Areas

Another disadvantage of the ellipse is that the ellipse can be made to infinity outside the figure. This gives a lot of room for error, because if an extremely large ellipse is drawn on one of the slices, the interpolation will no longer form to the natural shapes of the body. The three landmarks through which the ellipse should run on each slice is then also no longer achieved.

5.1.3 Tissue Labeling

The algorithms are created by testing the threshold values on the existing datasets. In the first place, one algorithm is designed to label the adipose tissue and another one is designed to label the non-adipose tissue. These algorithms are not enough, because the algorithms are not accurate enough when the the size of the breast differs. An algorithm should be developed to address relatively small breasts, considering lactating, non-lactating, adipose tissue, and non-adipose tissue. Additionally, these four variations of algorithms should also be created for relatively large breasts.

Besides these unique algorithms for smaller and larger breasts, the non-adipose tissue mainly consists of glandular tissue and blood vessels. For further research on lactation, it is important to distinguish these two tissue types. Therefore, with the volume of glandular tissue, relative proportions can be given to the different tissues in the breast related to breastfeeding.

5.1.4 Volume of the Labeled Tissues

Literature indicates that genetic factors and body weight influence breast volume. In this study, a correlation between weight and breast volume is noticed, despite the small amount of subjects. The two lightest subjects have the smallest breast volumes, the second heaviest subject has the second largest breast volume, and the heaviest subject has the largest breast volume.

For future research, it would be helpful to collect additional data such as BMI (Body Mass Index) and cup size, along with weight. This would provide a clearer understanding of whether the measured volumes are realistic.

5.1.5 Double Labeled Tissue

The presence of double-labeled pixels in mammary breast tissue suggests improving the algorithms. Adjustments in threshold and contouring variables could improve this process. In subjects 1, 2, and 4, labeled tissue appears mainly at tissue edges where adipose transitions to non-adipose tissue. The double-labeled tissue is within these three subjects under 7 %. However, in subject 3, with a 14% labeling rate, double labeling occurs not only at edges but also across larger areas. This indicates potential misrecognition of one of the tissues, where the algorithm could improve significantly.

It is noteworthy that in Figure 4.11 (c), there is a 41% presence of non-adipose tissue in the breast. Since this subject is not currently lactating, this percentage is considerably high compared to Subjects 1 and 4, who have 17% and 7% non-adipose tissue, respectively. This variation may be partly due to the high percentage of double-labeled tissue, suggesting that the algorithms applied may not be appropriate for this subject.

Additionally, numerous unlabeled black pixels are visible in mammary breast tissue, primarily at edges where non-adipose transitions to adipose tissue. This indicates that current variables may have overly high thresholds.

Future research could benefit from determining the total volume of mammary breast tissue to assess the extent of unlabeled pixels, which could substantially influence the volume estimates of different tissues.

5.2 Test of Protocol

The protocol worked well, which was reflected in the independence with which the testers performed the manual segmentation. This was despite the fact that it was the first time they had seen the protocol and had never practised segmentation before.
The results from the protocol testers were quite close, particularly for the non-adipose tissue, where the differences were small, around 10 mL. However, in adipose tissue, the differences were more significant, with 130 mL difference for subject 4 and 63 mL difference for subject 2. These larger differences in adipose tissue in comparison to non-adipose tissue are due to the manual segmentation process, which primarily masks tissue where it consists mostly of adipose tissue. The non-adipose tissue, especially glandular tissue, is located deeper in the breast and this is not the part of the breast where the tissue is cut off.

5.3 Comparison of Segmentation Methods

The results of the average volumes using Rozan's method compared to the average volumes of this study show differences of up to 230 mL. However, the smallest difference, seen in subject 4 with a range of only 6 mL, indicates the reliability of the methods developed.

It is important to note some methodological differences that influence the volumes shown in table 4.1. One important factor is that the method used in this study did not calculate the total breast volume, but only focused on adipose and non-adipose tissue separately. This leads to double-labeled tissues and non-labeled tissues within the mammary breast tissue.

In addition, other factors may have contributed to the differences in total volume. For example, different scan types were used (T1 and T2), Rozan's method excluded certain slices whereas this study did not and this method included 5 slices to draw the lines and points compared to Rozan's 3 slices.

6 CONCLUSION

A method to segment adipose and non-adipose tissue in the mammary breast has been successful. The segmentation process starts with drawing ellipses and points on five different slices to remove all non-mammary breast tissue from the figure. Between these 5 slices, intermediate slices are automatically interpolated using a smooth 'spline' interpolation function in MATLAB. This segmentation part shows a maximum variance of 6.7% in adipose tissue and 1.51% in non-adipose tissue, showing consistency. The second part of the segmentation utilizes the MATLAB Toolbox 'Medical Image Labeler' and a self-developed automated algorithm to distinguish adipose and non-adipose tissues using T2-Dixon Fat and Water scans. The algorithms could be improved to prevent double-labeling or not-labeled tissues within the mammary breast tissue.

The method developed in this project for calculating volumes of adipose and non-adipose tissue in the mammary breast produces realistic results, validated against volumes from another study on creating a segmentation method, using the same dataset. Comparisons show variances ranging from 0.15% to 14.4%.

7 OUTLOOK

Continuing this study, it is possible to validate whether the first two centimeters of a lactating breast, measured from the skin, is representative of the whole breast. To do this, it is not only necessary to quantify the proportions of adipose and non-adipose tissue in the whole breast, but also to determine the same proportions within the first 2 cm from the skin.

This can be achieved by modelling the breast contour in 3D and projecting a 2 cm smaller version of this shape perpendicular to the original contour into the breast. The tissue deeper than this 2 cm is then removed from the MR images, by making the pixels black. The remaining tissue can then be used to determine the proportions of adipose and non-adipose tissue in the first 2 cm of the lactating breast.

Based on the dataset of the lactating subject, it is expected that the first 2 cm of the breast is not representative of the whole breast. Figure 7.1 shows a slice of the dataset of the lactating subject where the non-pink area represents the first 2 cm of the breast. This image is a Dixon-Fat scan where the light tissue is adipose tissue and the dark tissue is non-adipose tissue (which largely includes glandular tissue and blood vessels). This observation suggests that the superficial layers of the breast may not have the same tissue proportions as the deeper layers. Visually, this 2 cm border is proportionally composed of more adipose tissue than the proportions of the whole breast. This would conclude that the DOSI scans are not qualified to show the correct proportions of adipose and non-adipose tissue. Further quantification and analysis is required to confirm this hypothesis and to determine the exact differences in tissue proportions. With these results, the field of lactation insufficiency research is one step closer to finding the cause.

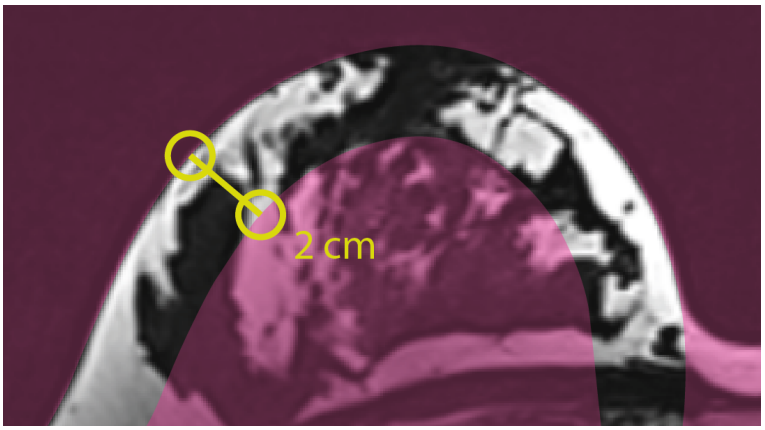

Figure 7.1: First two centimeter (non-pink area) of the lactating breast, measured from the skin

REFERENCES

[1] Katie L Westerfield, Kristen Koenig, and Robert Oh. Breastfeeding: Common Questions and Answers. *American family physician*, 98(6):368–373, 9 2018.

[2] Cesar G Victora, Rajiv Bahl, Aluísio J D Barros, Giovanny V A França, Susan Horton, Julia Krasevec, Simon Murch, Mari Jeeva Sankar, Neff Walker, and Nigel C Rollins. Breastfeeding in the 21st century: epidemiology, mechanisms, and lifelong effect. *The Lancet*, 387(10017):475–490, 1 2016.

[3] Colin Binns, MiKyung Lee, and Wah Yun Low. The Long-Term Public Health Benefits of Breastfeeding. *Asia Pacific Journal of Public Health*, 28(1):7–14, 1 2016.

[4] E.A. van der Wilk and C.I. Lanting. Zuigelingen die borst- of kunstvoeding krijgen 2018.

[5] Gianni, Bettinelli, Manfra, Sorrentino, Bezze, Plevani, Cavallaro, Raffaeli, Crippa, Colombo, Morniroli, Liotto, Roggero, Villamor, Marchisio, and Mosca. Breastfeeding Difficulties and Risk for Early Breastfeeding Cessation. *Nutrients*, 11(10):2266, 9 2019.

[6] NCJ Ondine Engelse and TNO Paula van Dommelen. Peiling Melkvoeding . *Nederlands Centrum Jeugdgezondheid*, 2018.

[7] Cecilia Peñacoba and Patricia Catala. Associations Between Breastfeeding and Mother-Infant Relationships: A Systematic Review. *Breastfeeding medicine : the official journal of the Academy of Breastfeeding Medicine*, 14(9):616–629, 11 2019.

[8] S H Chung, A E Cerussi, C Klifa, H M Baek, O Birgul, G Gulsen, S I Merritt, D Hsiang, and B J Tromberg. In vivo water state measurements in breast cancer using broadband diffuse optical spectroscopy. *Physics in Medicine and Biology*, 53(23):6713–6727, 12 2008.

[9] Vincent Kitsmiller, Thomas D. O'Sullivan, and Roy Stillwell. Toward handheld real time frequency domain diffuse optical spectroscopy. In Sergio Fantini, Paola Taroni, Bruce J. Tromberg, and Eva M. Sevick-Muraca, editors, *Optical Tomography and Spectroscopy of Tissue XIII*, page 5. SPIE, 3 2019.

[10] Magnetic Resonance Imaging (MRI).

[11] F. van Gameren. Improving the user interface of a 3D full breast photoacoustic tomography system. 188, 8 2021.

[12] H. Oldenburg and M. V. Peeters. *Alles over borstkanker*. Poiesz Uitgevers, 7de ed., vol. 2020 edition, 2007.

[13] Giovanni Bistoni and Jian Farhadi. Anatomy and physiology of the breast. In *Plastic and reconstructive surgery*, pages 477–485. Wiley, 4 2015.

[14] SONALI PANDYA and RICHARD G. MOORE. Breast Development and Anatomy. *Clinical Obstetrics & Gynecology*, 54(1):91–95, 3 2011.

[15] Fadil M. Hannan, Taha Elajnaf, Laura N. Vandenberg, Stephen H. Kennedy, and Rajesh V. Thakker. Hormonal regulation of mammary gland development and lactation. *Nature Reviews Endocrinology*, 19(1):46–61, 1 2023.

[16] Ma'mon M. Hatmal, Mohammad A. I. Al-Hatamleh, Amin N. Olaimat, Walhan Alshaer, Hanan Hasan, Khaled A. Albakri, Enas Alkhafaji, Nada N. Issa, Murad A. Al-Holy, Salim M. Abderrahman, Atiyeh M. Abdallah, and Rohimah Mohamud. Immunomodulatory Properties of Human Breast Milk: MicroRNA Contents and Potential Epigenetic Effects. *Biomedicines*, 10(6):1219, 5 2022.

[17] Galit Mimouni, Paul Merlob, Francis B. Mimouni, Alona Bin Nun, and Yair Kasirer. Nipple/Areola Dimensions in Early Breastfeeding. *Breastfeeding Medicine*, 17(6):506–510, 6 2022.

[18] Elaine N. Marieb and Katja Hoehn. *Human Anatomy & Physiology*. Pearson, tenth edition, 2016.

[19] Donna T. Geddes. Inside the Lactating Breast: The Latest Anatomy Research. *Journal of Midwifery & Women's Health*, 52(6):556–563, 11 2007.

[20] LRCB. ANATOMIE EN PATHALOGIE VAN DE MAMMA. *Dutch reference centre for screening*, 62, 8 2015.

[21] Dinesh Pandey, Xiaoxia Yin, Hua Wang, Min-Ying Su, Jeon-Hor Chen, Jianlin Wu, and Yanchun Zhang. Automatic and fast segmentation of breast region-of-interest (ROI) and density in MRIs. *Heliyon*, 4(12):e01042, 12 2018.

[22] Asma Javed and Aida Lteif. Development of the Human Breast. *Seminars in Plastic Surgery*, 27(01):005–012, 5 2013.

[23] Sandrine Truchet and Edith Honvo-Houéto. Physiology of milk secretion. *Best Practice & Research Clinical Endocrinology & Metabolism*, 31(4):367–384, 8 2017.

[24] Jerry L. Prince and Jonathan. M. Links. *Medical Imaging Signals and Systems*. Pearson, 2 edition.

[25] Suraj D. Serai. Basics of magnetic resonance imaging and quantitative parameters T1, T2, T2*, T1rho and diffusion-weighted imaging. *Pediatric Radiology*, 52(2):217–227, 2 2022.

[26] Mark W. Carr and Michael L. Grey. Magnetic Resonance Imaging: Overview, risks, and safety measures. *AJN The American Journal of Nursing*, 12 2002.

[27] Maike E. Lindemann, Mark Oehmigen, Titus Lanz, Hong Grafe, Nils Martin Bruckmann, Lale Umutlu, and Harald H. Quick. Evaluation of improved CT□based hardware attenuation correction in PET/MRI: Application to a 16□channel RF breast coil. *Medical Physics*, 49(4):2279–2294, 4 2022.

[28] Reza Salari, David H. Ballard, Mark J. Hoegger, Daniel Young, and Anup S. Shetty. Fat-only Dixon: how to use it in body MRI. *Abdominal Radiology*, 47(7):2527–2544, 7 2022.

[29] Jingfei Ma. Dixon techniques for water and fat imaging. *Journal of Magnetic Resonance Imaging*, 28(3):543–558, 9 2008.

[30] Breast 18 coil.

A INTERPOLATION ON DIXON-FAT IMAGES

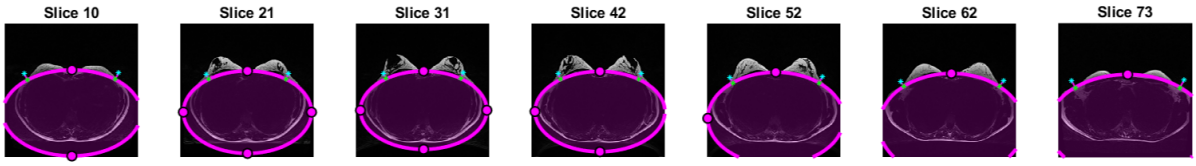

Figure A.1: First step of segmentation on subject 1

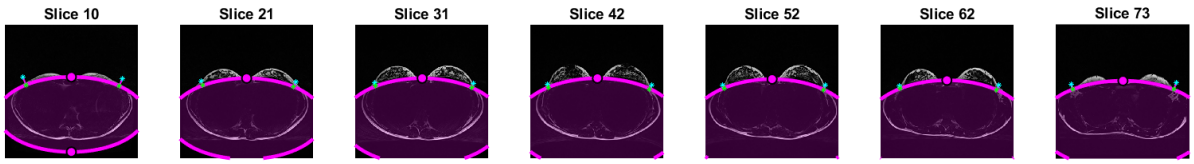

Figure A.2: First step of segmentation on subject 3

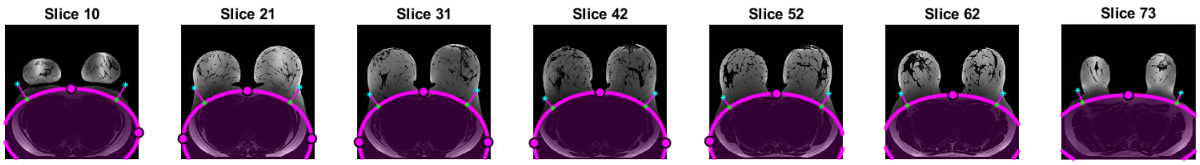

Figure A.3: First step of segmentation on subject 4

B INTERPOLATION ON DIXON-WATER IMAGES

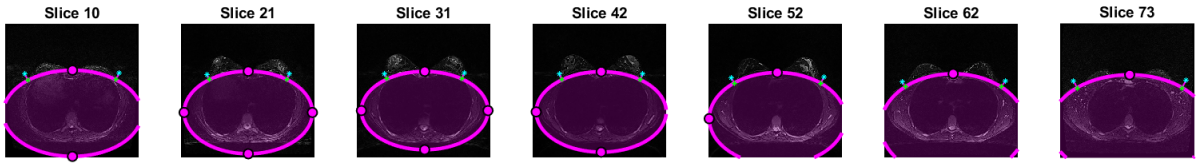

Figure B.1: First step of segmentation on subject 1

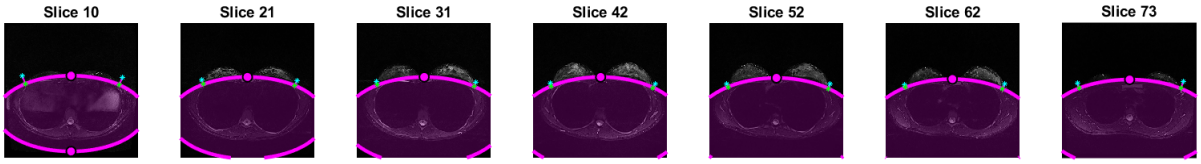

Figure B.2: First step of segmentation on subject 3

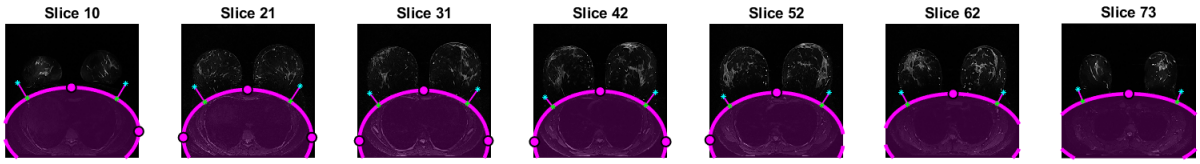

Figure B.3: First step of segmentation on subject 4

C PROTOCOL

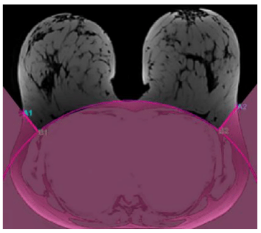

Protocol borstsegmentatie

Doel van dit protocol: Het juist segmenteren van de borst met behulp van een Matlab script, waarna er alleen borstweefsel over zal blijven in de afbeelding.

Stap 1:
Open Matlab (het liefst versie r2024a) en ga naar: \\ad.utwente.nl\org\TNW\BMPI\Patientdata\Lactation project – Breast MRI\Lonneke . Open het bestand: “Script_segmentatie_fat.m”

Stap 2:
Druk op 'Run' onder het kopje Editor. De foto’s worden ingeladen, dit duurt ongeveer 20 seconden.

Stap 3:
Voer de naam van het bestand in, ‘Proefpersoon2_DixonFat’ (dit is hoofdletter gevoelig). Voer jouw eigen voornaam in en druk op ‘OK’. Bij het starten van het script wordt de eerste slice van een 3D map met 83 foto's geladen. Je gaat in totaal vijf slices intekenen: één bij de eerste slice, één op een kwart, één op de helft, één op driekwart, en één bij de laatste slice.

Stap 4:
De eerste afbeelding komt in beeld en je kunt beginnen met het intekenen van een ellips. De ellips is bedoeld om alles wat binnen de ellips valt zwart te maken. Het doel is om alleen het borstweefsel over te houden en de rest van de borstkas handmatig te verwijderen.

Druk de muisknop in vanaf het meest linker deel van het lichaam, naar het meest rechter deel. Zorg ervoor dat de ellips zo min mogelijk roteert (als de ellips te veel roteert, kun je deze terug roteren door op het bovenste bolletje van de ellips te klikken en te slepen). Kijk vervolgens naar de positie van de ellips en verschuif/vervorm de ellips voor zover je wilt. Bij de eerste afbeelding is er nog geen borstweefsel te zien op de figuur. De gehele borstkas moet bedekt worden met de ellips, want alles wat in de ellips staat wordt zwart gemaakt. Hieronder is een voorbeeld te zien.

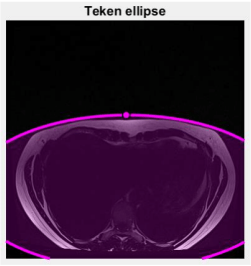

Het belangrijkste is dat al het weefsel binnen de ellips valt. Aan de bovenkant van het lichaam moet de rand van de ellips dicht bij de rand van de borstkas liggen. Aan de onderkant komt het wat minder precies (zolang al het weefsel maar in de ellips valt) en het mag lekker ruim genomen worden. Als je tevreden bent met hoe de ellips loopt, kan je dubbelklikken op de rand van de ellips. De ellips is nu opgeslagen.

Stap 5:
Nu is het tijd om de twee losse punten in te tekenen. Deze eerste afbeelding is een uitzondering, omdat er geen borstweefsel in beeld is. Er zullen nog wel punten moeten worden ingetekend. Deze moeten ter hoogte komen van het hoogste punt van de door jou ingetekende ellips. Het linker punt (het eerste punt die gezet moet worden) moet vervolgens in lijn komen met het meest linker punt van de borstkas. Het rechter punt (het tweede punt die gezet moet worden) moet in lijn komen met het meest rechter punt van de borstkas. De punten zijn pas zichtbaar als ze allebei zijn ingetekend, één klik per punt is dus genoeg. Een voorbeeld van deze punten is te zien in de figuur hieronder als A1 en A2. B1 en B2 worden vervolgens automatisch gevormd.

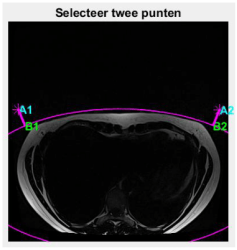

Stap 6:
Er komt meteen een nieuwe afbeelding in het scherm, waarin eerst weer een ellips mag worden getekend. Er is nu ook borstweefsel aanwezig, dus de ellips moet nu door de onderstaande drie punten lopen (die aangegeven zijn in oranje in de figuren hieronder).

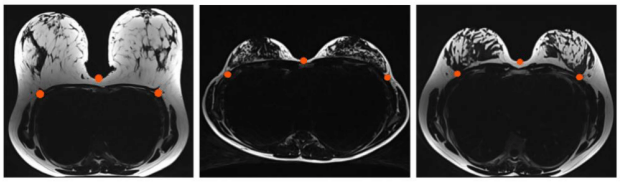

De buitenste twee punten zijn te herkennen aan een licht-aangekleurd weefsel, wat een hoekig lijkt (deze positie is makkelijker te vinden met behulp van de oranje punten hierboven). Het middelste punt is het hoogste punt van het lichaam tussen de twee borsten in. Een voorbeeld van de juiste positionering van de ellips is hieronder te zien.

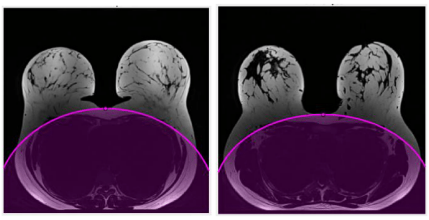

Zodra je tevreden bent met hoe de ellips loopt, kun je deze opslaan door dubbel te klikken op de rand van de ellips.

Stap 7:
Nu is het tijd om de twee losse punten in te tekenen. Deze twee punten moeten geplaatst worden op de holle posities aan de laterale zijde van de borsten (buitenzijden), zoals aangegeven met de paarse punten in de onderstaande figuren. Het is belangrijk om altijd het eerste punt links te plaatsen en het twee punt rechts. In sommige gevallen kan de hoek moeilijk te bepalen zijn. Kies in dergelijke gevallen het middelste punt van het meest "rechte" segment, zoals in de meest rechter figuur hieronder is gedaan. De punten zijn pas zichtbaar als ze allebei zijn ingetekend, één klik per punt is dus genoeg.

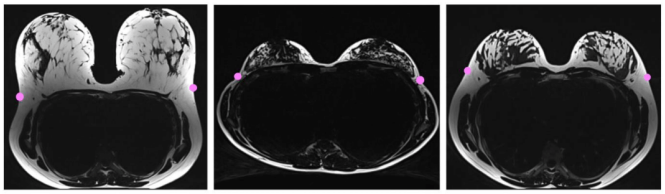

Uiteindelijk zullen de stukken weefsel dat aan de buitenzijden zit, gemaskeerd door de lijnen en de ellips, ook zwart worden gemaakt. Hieronder wordt weergegeven in het roze wat weg wordt gehaald.

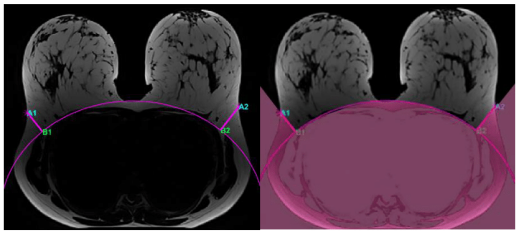

Stap 8:
Herhaal stap 6 en 7 voor de volgende 2 afbeeldingen.

Stap 9:
Nu is de laatste afbeelding in beeld gekomen. Hierop is wederom geen borstweefsel te zien, dus de gehele borstkas mag weer omlijnt worden door de ellips, zoals hieronder te zien is. De bovenrand moet dicht bij de bovenrand van het lichaam worden geplaatst. De onderkant van de ellips mag weer ruim genomen worden.

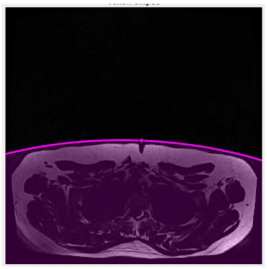

Stap 10:
De twee punten mogen nu weer getekend worden, waarvan het eerste punt links en het twee punt rechts. Omdat er geen borstweefsel te zien is, mogen de punten ter hoogte van het hoogste punt van de ellips komen te staan. Het linker punt (het eerste punt dat geplaatst moet worden) moet vervolgens in lijn komen met het meest linker punt van de borstkas en het rechter punt (het tweede punt dat geplaatst moet worden) moet in lijn komen met het meest rechter punt van de borstkas. Als het meest linker en rechter deel van het lichaam niet te zien zijn, mogen de punten dicht bij de uiteindes van de foto worden geplaatst. De punten zijn pas zichtbaar als ze allebei zijn ingetekend, één klik per punt is dus genoeg.

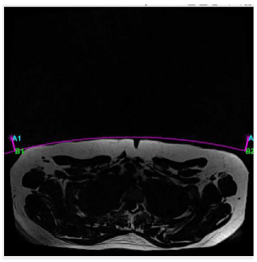

Stap 11:
Als de 5e afbeelding is ingetekend, zal Matlab de rest doen. De nieuwe DICOM folder met gemaskeerde figuren wordt opgeslagen en ondertussen zal er een 'gif' worden laten zien met de gemaskeerde figuren voor elke slice.

Stap 12:
Herhaal alles vanaf stap 2 om ook voor proefpersoon 4 ('Proefpersoon4_DixonFat') de ellipsen en punten in te tekenen.